

**Adsorption-induced conformational changes in protein diffusion-aggregation surface assemblies**Delphine Pellenc,<sup>1</sup> Olivier Gallet,<sup>1</sup> and Hugues Berry<sup>1,2,\*</sup><sup>1</sup>*ERRMECe, Université de Cergy-Pontoise, 2 avenue Adolphe Chauvin, 95302 Pontoise Cedex, France*<sup>2</sup>*Team Alchemy, INRIA Futurs, 4, rue Jacques Monod, 91893 Orsay Cedex, France*

(Received 22 May 2005; revised manuscript received 1 August 2005; published 2 November 2005)

Two-dimensional rigid colloid aggregation models may be applied to protein layers when no large conformational change is involved. Yet, following adsorption, several proteins undergo a conformational transition that may be involved in aggregative structures. Our focus here is how a conformational change might influence surface clustering in a diffusion-aggregation model. We propose a model including diffusion, aggregation, and unfolding of proteins that are randomly adsorbed onto a surface. Our model allows simulating the case where protein-protein interaction favors unfolding and the case where this interaction prevents it. We study the effect of a simple disk-to-rod unidirectional unfolding and investigate the morphology of the resulting clusters in the diffusion- and reaction-limited regimes. A rich variety of structures is produced, with fractal dimension differing from that in universal diffusive aggregation models. Increasing unfolding probability shifts the system from the neighbor-induced to the neighbor-prevented unfolding regime. The intermediate structures that arise from our model could be helpful in understanding the assembly of different observed protein structures.

DOI: [10.1103/PhysRevE.72.051904](https://doi.org/10.1103/PhysRevE.72.051904)

PACS number(s): 87.68.+z, 82.40.Np, 87.14.Ee, 87.15.Aa

**I. INTRODUCTION**

Proteins may be found circulating, in physiological fluids, incorporated in a gel, in the extracellular matrix (ECM), or interacting with solid surfaces. This is the case in bone and teeth where ECM proteins are closely associated with the mineral matrix. This interaction plays a direct role in the mineralization process [1–4] and has been focused on in several studies [5–11]. The surface-protein interaction is also one of the first events following an implant graft and raises much interest in biomedical engineering [12–17].

Protein layer functions depend on both the single molecule conformational state and the self-assembled structure properties. The conformation of a protein depends on its location and surrounding, and adsorption at interfaces may strongly affect it. A protein may indeed undergo surface-induced conformational changes, often referred to as “surface denaturations” [18,19]. In several cases, these transitions lead to conformations that have functions differing from those of the soluble forms. They may for instance result in a loss of activity for enzymes [20,21], or in the modulation of the adhesion-promoting effect of ECM proteins [22,23]. The properties of a protein layer depend not only on the molecule conformation but also on the spatial distribution of the proteins on the surface [24] which may prevail over substrate topology [25]. Maheshwari *et al.* have, for instance, shown that, at a given surface density of adhesion-promoting peptides, cell adhesion, cytoskeleton organization, and migration speed tend to be favored by a clustered distribution of the peptides, with respect to their dispersion over the surface [26].

Given the tight correlation between protein layer morphology and function, the accurate understanding and prediction of their morphological features appears to be needed in

various areas of biology. In that perspective, simulation studies may be a useful tool and several approaches have been developed over the past decade.

Surface assembly of sphere-shaped particles are well described by diffusion aggregation models derived from Witten and Sanger’s model [27] and adapted to random sequential adsorption processes [28]. Briefly, in this kind of model, once adsorbed, particles diffuse randomly onto the surface and two particles may aggregate when meeting one another. Those models are able to describe protein surface assemblies in different bulk conditions provided the adsorption does not induce a large conformational change [29]. It is known though that a number of protein aggregative structures, such as fibrils, the assembly of which may be surface induced [30], imply partial unfolding [31–34]. Van Tassel *et al.* developed a sequential adsorption model that includes a symmetrical postadsorption conformational change of the molecule [35]. This model fits fibronectin adsorption data in terms of kinetic behavior or surface coverage but does not include surface diffusion. However, their more recent data suggest a postadsorption clustering that might involve surface diffusion [36,37].

Considering the experimental knowledge of protein adsorption, a model of protein layer formation should take both surface diffusion and unfolding of the adsorbed protein into account. Our focus here is how conformational changes might influence the protein surface clustering process in a diffusion-aggregation model and thus the morphology of the resulting surface assemblies. We propose a model including diffusion, aggregation, and unfolding of molecules that are randomly adsorbed onto a surface. We study the effect of a simple unidirectional unfolding from a disk- to a rod-shaped particle. Unfolding is first considered not to depend on the vicinity of the protein. We also study the effects of protein-protein interactions on the unfolding events. We investigate the role of unfolding on the morphology of the resulting clusters in both the diffusion-limited (DL) and reaction-limited (RL) regimes.

\*Corresponding author. Electronic address: [hugues.berry@inria.fr](mailto:hugues.berry@inria.fr)

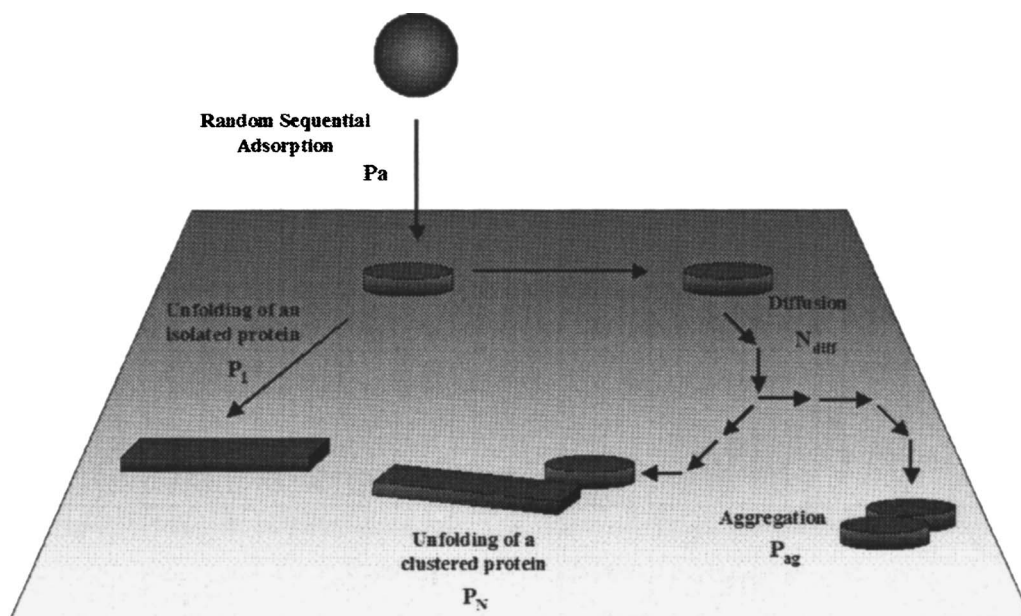


FIG. 1. Depiction of the model. At each time step, proteins adsorb at a random position. They are then allowed to diffuse on the surface unless they unfold or aggregate. Neighbor-required unfolding  $P_I=0$ ; neighbor-prevented unfolding  $P_N=0$ ; neighbor-independent unfolding  $P_I=P_N$ .

## II. MODEL AND SIMULATION PROCEDURES

Bulk proteins are modeled as disk-shaped particles of radius  $\alpha$  that adsorb onto a square lattice of size  $L \times L$  at random positions. Figure 1 shows a general scheme of the model. At each adsorption step, representing  $1/L^2$  time step, a position for the center of a particle is chosen at random and, provided adsorption results in no overlap with previously adsorbed proteins, the protein adsorbs with a probability  $P_a$ . All the adsorbed proteins are then allowed to diffuse according to an  $N_{diff}$ -step random walk of their particle centers. We consider the diffusion of a cluster to be slow enough to be negligible and let only monomers diffuse so that the aggregation of a protein results in its immobilization. If a protein diffuses beyond the lattice limits, it is removed. The boundary conditions had no influence on the results due to a large system size. We include unfolding attempts of the adsorbed protein between adsorption events. If allowed to, the protein will then spread into a rodlike particle. The unfolding maximizes the contact between the protein and the surface which increases the binding energy. The unfolded species is therefore often considered irreversibly adsorbed [38,39]. Consistent with this view, we considered the unfolded protein diffusion to be negligible. If two proteins come in contact, i.e., when at least two sites of theirs become nearest neighbors, they have a probability  $P_{ag}$  to irreversibly aggregate.

To study the effect of protein interactions on the conformational change, the unfolding of an isolated molecule and that of a protein that is part of a cluster are considered separately. Unfolding of an isolated protein occurs symmetrically from the center of the molecule while unfolding of a clustered protein starts from the contact site with the neighbor. Both undergo excluded surface effects and the direction of

unfolding is chosen at random among available ones. These two events are referred to as isolated and neighbor-induced unfolding with respective probabilities  $P_I$  and  $P_N$  per protein per unit time. The case  $P_I=0$  stands for neighbor-required and  $P_N=0$  for neighbour-prevented unfolding. Hence,  $P_I=P_N$  represents a neighbour-independent unfolding.

Each simulation is performed on a square lattice of linear dimension  $L=1500$ . The folded proteins are modeled as disk-shaped particles of radius  $\alpha=3$  and the unfolded ones as rods of length  $\beta=29$  and thickness 1. Note that  $\beta$  is taken to keep constant the number of sites occupied by a single protein whether it is unfolded or not. The fractal dimension of deposition-diffusion-aggregation models is known to depend on the relative values of the deposition flux and the diffusion coefficient, as well on the surface coverage [28,40,41]. We found the ratio  $P_a/N_{diff}=10^{-6}$  to allow the generation of isolated clusters in the diffusion-limited regime that are similar in aspect and fractal dimension to the diffusion-limited aggregation (DLA) and reaction-limited aggregation (RLA) clusters when no unfolding takes place. To investigate the effect of the unfolding with respect to these well known DLA and RLA structures, all the simulations are therefore performed with  $P_a=10^{-4}$  and  $N_{diff}=100$ . One should note here, that, the minimal rate parameters of the model are  $N_{diff}/P_a$ ,  $P_{ag}$ ,  $P_I/P_A$ , and  $P_N/P_A$ . The simulations are completed for a final surface coverage  $\theta$  much below the percolation threshold,  $\theta \sim 0.013$ , that is, for 1000 proteins being present on a lattice of size  $L=1500$ , at the same time. We specifically study the cases  $P_{ag}=1$  and  $10^{-3}$ . For reading convenience, we refer to these cases as the DL and RL regimes even when the unfolding shifts the systems to other behavior. The fractal dimensions of the resulting clusters are estimated using a box counting method [42].

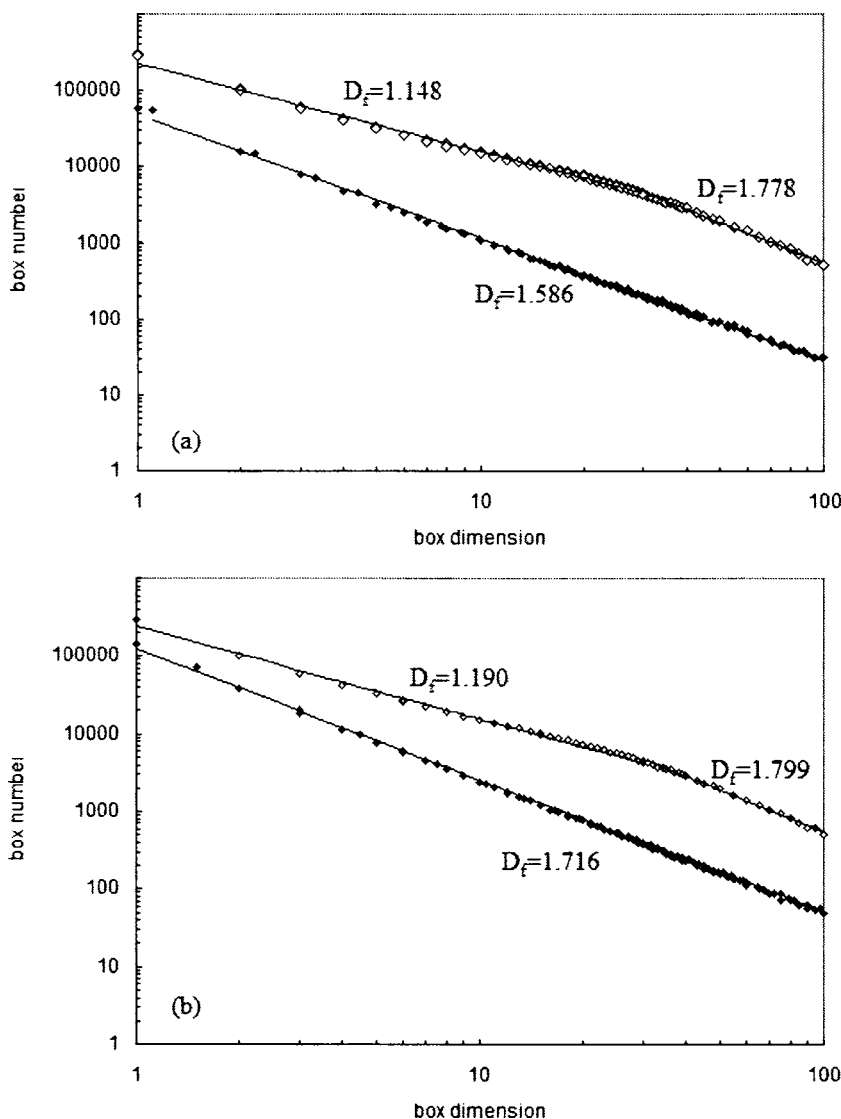


FIG. 2. Illustration of the cluster fractal dimension calculation using a box counting method. The fractal dimension  $D_f$  is deduced from the slope of the log-log plot of the number of boxes versus the box dimension. Two unfolding probabilities are shown here,  $P=1$  (open symbols) and  $10^{-7}$  (filled symbols), in the case of neighbor-independent unfolding, i.e.,  $P_N=P_I$ . (a) Diffusion-limited regime,  $P_{ag}=1$ ; (b) reaction-limited regime,  $P_{ag}=10^{-3}$ . For  $P=1$  a two-scale behavior is observed, so that each part of the curve is fitted independently and the two corresponding dimensions are indicated. In both panels, the curves have been shifted for clarity.

III. RESULTS AND DISCUSSION

We investigated the effect of the unfolding of the monomer on the morphology of surface protein clusters. We studied separately the effects of the neighborhood and of the surface on the unfolding. This can be done by dissociating the unfolding probability into a surface-induced unfolding probability  $P_I$  when the protein is isolated, and a neighbor-induced probability  $P_N$  when it is in contact with another one. The case  $P_I=0$  represents neighbor-required unfolding,  $P_N=0$  neighbor-prevented unfolding, and  $P_N=P_I$  neighbor-independent unfolding. All the simulations are performed for the same final surface coverage and the folded and unfolded monomers cover the same surface fraction. This allows us to study the only effect of the conformation change on the cluster morphology.

The clusters exhibit autosimilarity properties as shown by the power-law behavior of the number of square boxes needed to cover a cluster vs the box linear dimension plotted in Fig. 2. This allows us to compare their morphology in terms of fractal dimension, over the whole range of unfolding probabilities studied here. At high unfolding probability,

in both neighbor-independent and neighbor-prevented unfolding, a two-scale behavior is observed, the first part of the curve reflecting the fractal dimension of small-sized clusters and the second, at larger length scales, reflecting a uniform distribution of these small clusters (Fig. 2). In the following, only the short-length scale fractal dimension, reflecting the cluster morphology, will be considered, when such behavior is observed.

Figure 3 shows the dependence of the cluster aspect and fractal dimension on the unfolding probability  $P$  in the diffusion-limited regime (i.e.,  $P_{ag}=1$ ). In this regime, setting both unfolding probabilities to zero generates clusters with fractal dimension of  $1.652 \pm 0.039$  (not shown), i.e., classical DLA on a two-dimensional square lattice [27]. When neighbor-required unfolding [Fig. 3(a)] is included, the clusters exhibit a ramified morphology that is close to DLA clusters at low  $P$ , but rapidly displays less compact structures, containing void spaces. Consistent with their aspect, the cluster fractal dimension decreases with increasing  $P$  to reach the average value  $1.431 \pm 0.025$  at  $P=10^{-5}$ , and no further change in the dimension is observed at higher probability. Even at low unfolding probability ( $1.640 \pm 0.011$  at  $P_N$

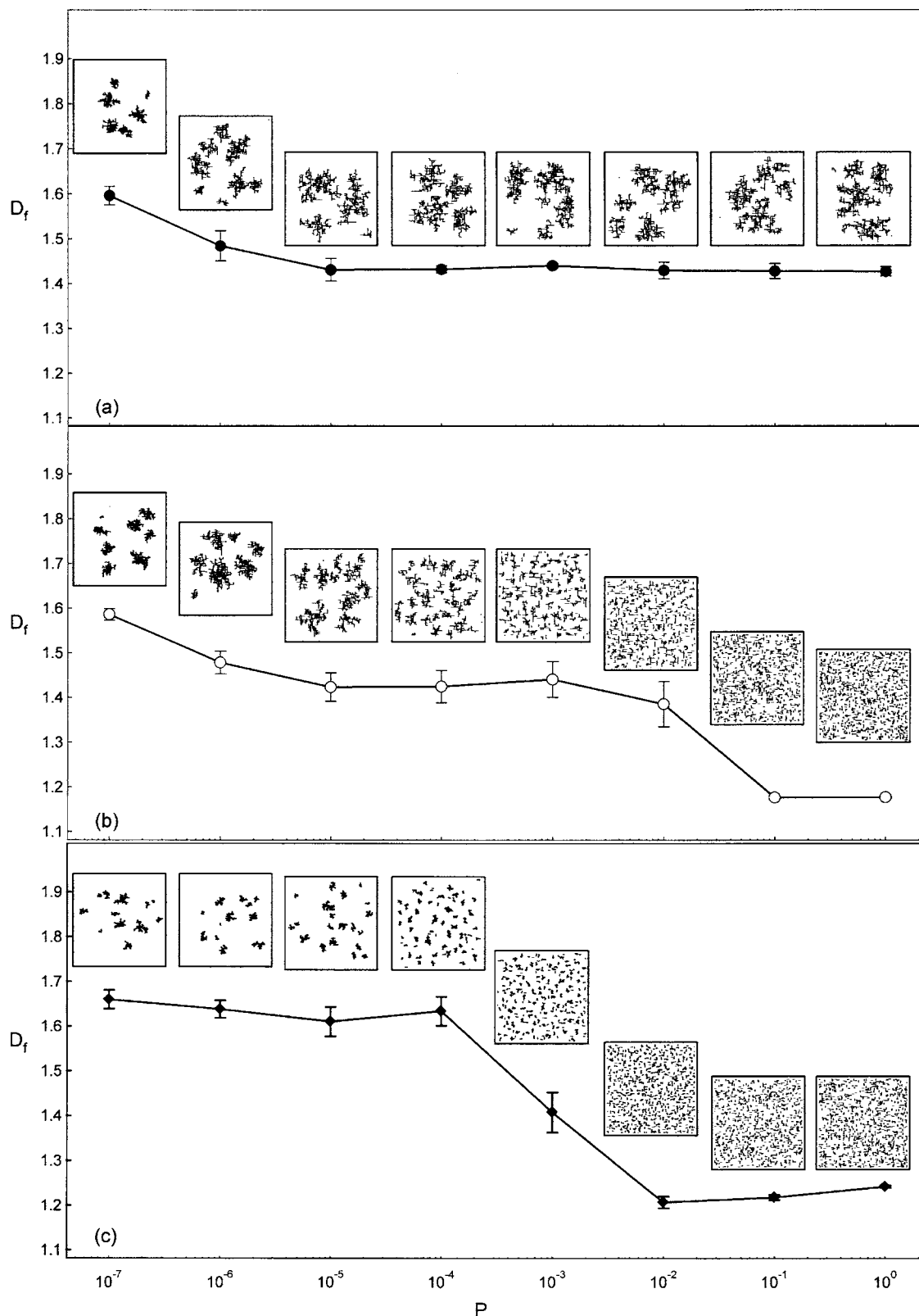


FIG. 3. Cluster fractal dimension  $D_f$  versus the unfolding probability  $P$  in the diffusion-limited regime where  $P_{ag}=1$ . (a) Neighbor-required unfolding,  $P=P_N$  and  $P_I=0$ ; (b) neighbor-independent unfolding,  $P=P_N=P_I$ ; and (c) neighbor-prevented unfolding,  $P=P_I$  and  $P_N=0$ . The insets on top of each plot show examples of lattice configurations for each parameter set.

$=10^{-7}$ ), the fractal dimension is significantly lower than the dimension found for the universal diffusive aggregation model. Unfolding causes a large cluster tip expansion, due to

the rod shape of unfolded proteins, and this allows the cluster to be reached from farther away by incoming proteins. This causes a faster growth, which, combined with the formation



of closed structures that prevents incoming proteins from diffusing inside the clusters, may explain the conformational-change-induced compactness decrease and corresponding low dimension. Cluster fractal dimensions lower than the DLA cluster dimension may also appear with spherical objects when cluster diffusion [43] or attractive interactions [44] are taken into account.

The aggregative behavior of diffusing rod-shaped particles have been studied in two [45,46] and three dimensions [47]. These studies showed that the larger the length of a particle, the higher the cluster fractal dimension. In the two-dimensional model, the orientations of the rod-shaped particles are all the same and remain fixed during the diffusion-aggregation process. Therefore, the increase of the fractal dimension simply results from the obligatory parallel packing of the rods. In the three-dimensional case though, the rods are initially randomly oriented and then diffuse in a direction depending on their aspect ratio. In this case, the increase of the fractal dimension is thought to arise from the possible aggregation of rods at distances lower than their larger gyration radius [47]. The apparent discrepancy of these results from ours might originate from the aggregative behavior of anisotropic objects that may vary with the Euclidean dimension. Our lower fractal dimension results from the monomer shape together with the fact that the unfolding produces closed structures, or loops, preventing incoming proteins from diffusing inside the clusters. If a similar loop is formed in three dimensions, incoming rods may still diffuse and reach the inner part of this kind of void. Either by “capping the void” (the axis of the incoming rod being in the plane of the void) or by crossing through it, this aggregation will increase the cluster fractal dimension. Such events, which are not allowed in our model, may in part explain why the fractal dimension decreases in two-dimensional (2D) rod clusters and increases in 3D.

In the case of neighbor-prevented unfolding, the clusters exhibit the typical morphology of DLA clusters at low  $P$  and little change, but a size decrease, is observed with increasing  $P$ . The fractal dimension shows no change either until  $P = 10^{-4}$  [Fig. 3(c)]. Above this value, it rapidly decreases to reach a plateau value of about 1.22. At high  $P$  values, the clusters actually mostly consist of monomers and dimers, and when  $P$  is 1, the network tends toward random sequential adsorption (RSA) of rodlike particles since almost no diffusion takes places and—except for steric considerations—all the proteins are unfolded.

When the unfolding does not depend on the monomer surroundings, i.e., for neighbor-independent unfolding, the fractal dimension shows a first decrease with increasing unfolding probability  $P$  and reaches a plateau value of  $\sim 1.43$  between  $10^{-5}$  and  $10^{-3}$  [Fig. 3(b)]. This decrease is very similar to that observed for neighbor-required unfolding [i.e.,  $P_I=0$ , Fig. 3(a)]. The cluster morphologies are very similar as well. It seems therefore that  $P_I$  does not play a significant role when little unfolding occurs. A second decrease is observed above  $10^{-3}$  until a final value of  $\sim 1.18$ , where the lattice configuration is close to random sequential adsorption. Cluster morphology crosses over from neighbor-required unfolding, at low  $P$  value, to neighbor-prevented unfolding at high  $P$  value. The transition occurs for unfold-

ing probabilities between  $10^{-4}$  and  $10^{-2}$ , where the fractal dimension is  $\sim 1.43$  in the three cases (neighbor-required, -prevented, and -independent unfolding). The clusters present, however, quite different morphologies. For neighbor-independent unfolding, with  $P=10^{-3}$  and  $10^{-2}$ , the dimension reflects the dimension of small-size clusters among which a few present an elongated, low-ramified structure. This may be understood in terms of steric effects. If two clusters grow close to one another, the direction of unfolding for a protein joining one of the cluster will be biased by the closest cluster. The neighbor-prevented unfolding probability decreases the distance between two cluster origins and this steric hindrance has a high probability to occur. In neighbor-required unfolding, the clusters are far enough from one another not to feel their neighbor [Fig. 3(a)] but close clusters, that do not bridge, do not interpenetrate much. This might thus suggest that the same steric effect is experienced on the cluster perimeter. Incidentally, one may think this simply occurs when the distance between two clusters becomes of the order of twofold the length of the unfolded protein.

In the reaction-limited regime (i.e.,  $P_{ag}=1$ ; Fig. 4), cluster morphologies that are very different from those observed in the diffusion-limited regime (Fig. 3) are generated. The neighbor-required unfolding produces dense clusters at  $P = 10^{-7}$ , with continuous compactness decrease with increasing  $P$ , while the neighbor-prevented unfolding leads to dense clusters close to RLA ones at low  $P$ , with size decrease until  $P=10^{-4}$ , beyond which the lattice resembles RSA configurations. The neighbor-independent unfolding clusters resemble neighbor-required unfolding ones at low  $P$  and neighbor-prevented unfolding ones at high  $P$ , with a specific intermediate morphology at  $P=10^{-5}$  and  $10^{-4}$ . The fractal dimension exhibits the same qualitative behavior with respect to unfolding probability as in the DL regime, i.e., an early slight decrease with  $P_N$  [Fig. 4(a)], and a later sharp decrease with  $P_I$  [Fig. 4(c)]. When both unfoldings are equally applied, the fractal dimension undergoes a two-step decrease with  $P$ , reflecting separate  $P_N$  and  $P_I$  influences [Fig. 4(b)]. As expected, the cluster dimension is overall higher than in the DL regime, except at high surface-induced unfolding value, where both regimes converge toward random sequential adsorption. Apart from cluster compactness, the RL regime also differs from the DL one regarding the crossover between neighbor- and surface-induced unfoldings, which occurs faster and at lower unfolding probability. By definition, in the RL regime, the monomers are not entirely sticky so that the proteins may jump back after a contact. Folded proteins are therefore statistically more often found isolated than interacting with another protein, at least at low surface coverage. No wonder then, if, in this regime, the crossover to isolated unfolding is found at lower unfolding probability value. In terms of protein adsorption, slowly aggregative proteins, which experience repulsive interactions, would tend rapidly toward random adsorption with increasing protein surface affinity.

The changes in fractal dimension observed when increasing the unfolding probability appear to be only partly correlated to the average proportion of unfolded protein per cluster as shown in Fig. 5. For both RL and DL regimes, in the neighbor-required unfolding case, the unfolded protein frac-

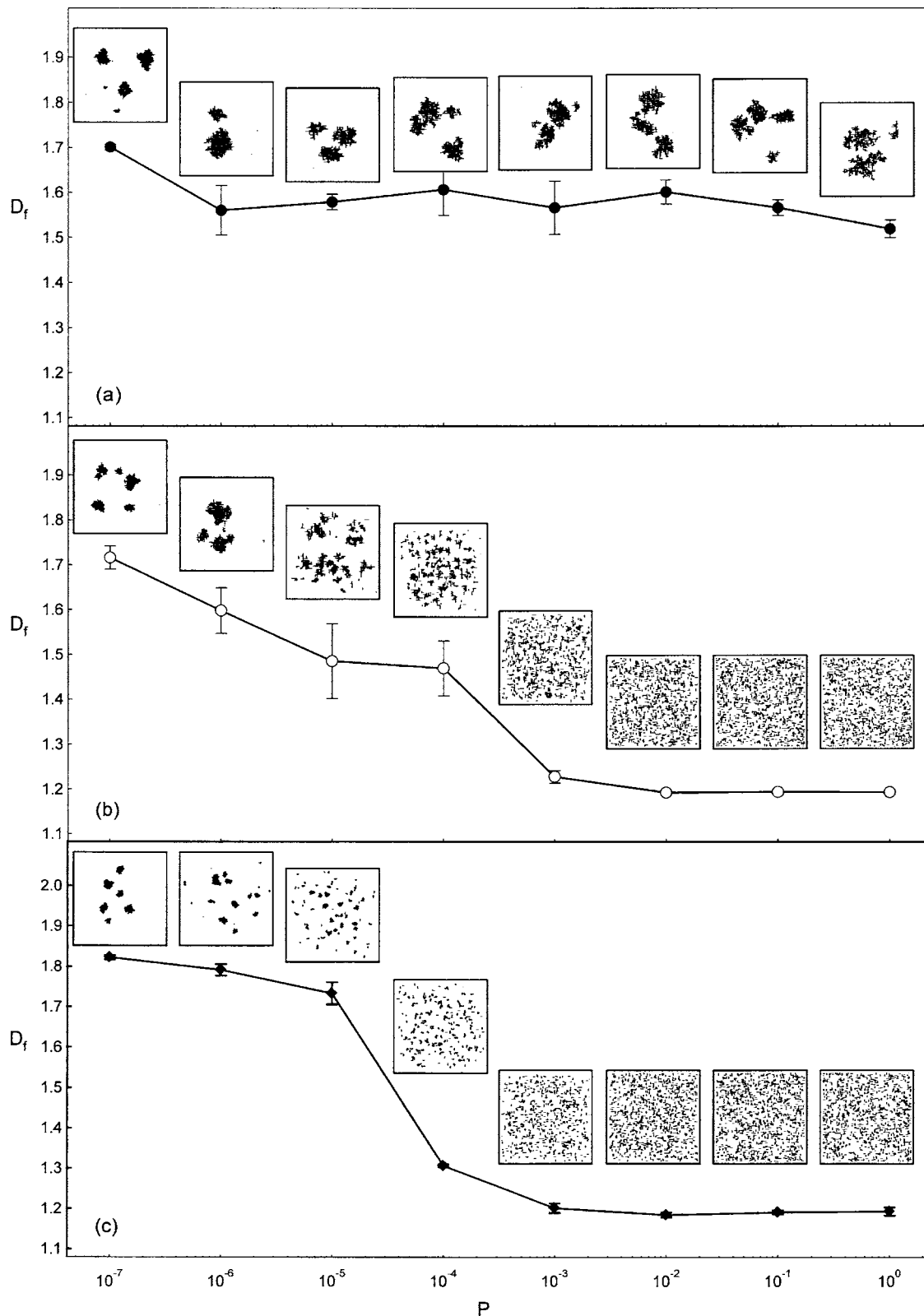


FIG. 4. Cluster fractal dimension  $D_f$  versus the unfolding probability  $P$  in the reaction-limited regime where  $P_{ag}=10^{-3}$ . (a) Neighbor-required unfolding,  $P=P_N$  and  $P_I=0$ ; (b) neighbor-independent unfolding,  $P=P_N=P_I$ ; and (c) neighbor-prevented unfolding,  $P=P_I$  and  $P_N=0$ . The insets on top of each plot show examples of lattice configurations for each parameter set.

tion slightly increases from  $10^{-7}$  to  $10^{-5}$ , above which it reaches its maximum value. For neighbor-prevented unfolding, it remains below 0.04 until  $10^{-4}$  and  $10^{-5}$  in the RL and

DL regimes, respectively, and then constantly increases. These behaviors reflect the changes observed in cluster fractal dimension for both regimes [Figs. 3, 4(a), and 4(c)]; the

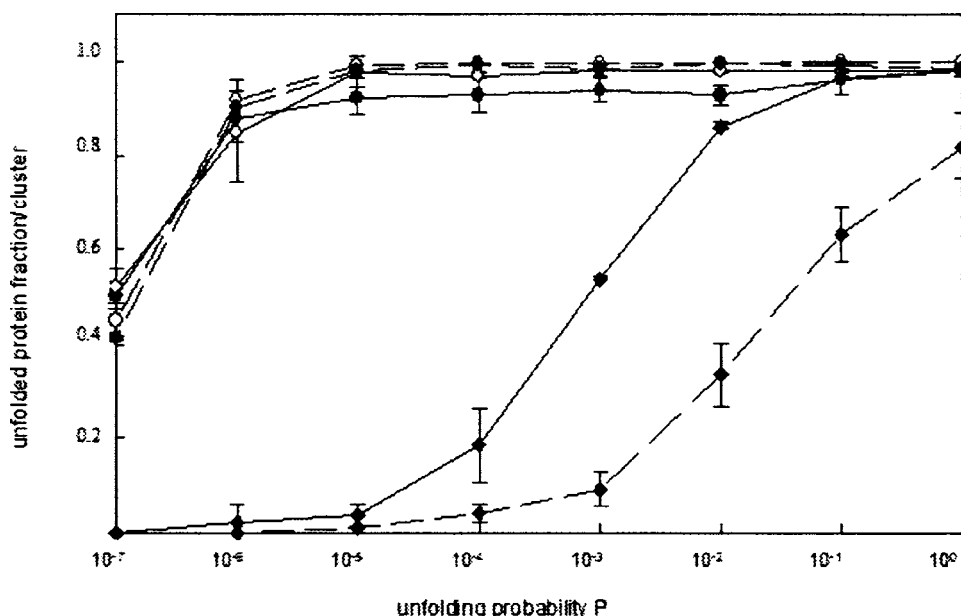


FIG. 5. Unfolded protein fraction per cluster versus unfolding probability  $P$  in the reaction- (continuous lines) and diffusion- (dotted lines) limited regimes for neighbor-prevented, -required, and -independent unfoldings. The symbols are the same as in Figs. 3 and 4. All curves exhibit the same shape except in the neighbor-prevented regime ( $P=P_j$ ;  $P_N=0$ ; filled diamonds) where the unfolded fraction increases more slowly with  $P$  in both regimes..

higher the unfolded fraction the lower the dimension. In the neighbor-prevented case, the unfolded fraction changes reflects the observed differences between the RL and DL regimes as well. Yet the correlation is not obvious for neighbor-independent unfolding. In this case, contrary to what is observed for the fractal dimension, the unfolded fraction does not exhibit an intermediate behavior between neighbor-prevented and -required unfoldings but rather follows neighbor-required unfolding behavior. The fact that the same unfolded fraction leads to a lower cluster fractal dimension when isolated unfolding is allowed suggests that the morphology of the resulting clusters depends not only on the unfolded fraction but also on whether these unfolding events occurs before or after the aggregation, i.e., whether they are isolated or clustered unfoldings.

In our model, we considered the diffusion of unfolded proteins to be negligible; hence, the higher the unfolding probability the shorter the diffusion length. Since cluster diffusion is negligible as well, unfolding only alters diffusion for isolated proteins. More than ending their diffusion, it also creates a new obstacle on the lattice for other diffusing proteins and subsequently increases the rate of aggregative encounters. At low unfolding probability, most of the proteins may diffuse and aggregate to a small number of clusters and unfolding of clustered proteins is favored. The higher the unfolding probability, the higher the number of clusters, so that proteins mostly form dimers and the system finally tends to a random sequential adsorption of rod particles, where almost no diffusion takes place. Between the two behaviors, the unfolding of isolated monomers is high enough to increase the cluster number and thus favor neighbor-induced unfolding, and low enough to allow diffusion and subsequent aggregation. It may therefore be supposed that the transition zone would be found at lower values the lower the diffusion coefficient of folded monomers.

**IV. RELEVANCE TO PROTEIN AGGREGATION**

We developed a deposition-diffusion-aggregation model that accounts for the adsorption-induced conformational

change, which is a generic feature of proteins at interfaces. Though widely described in experimental studies, this unfolding event has, however, seldom been considered in theoretical ones [35,38]. We aim at investigating conformational changes related to biomacromolecule surface self-assembly. For this purpose, we studied the effect of a very simple disk-to-rod transition of proteins adsorbing and diffusing on a lattice.

Proteins undergo various structural changes upon adsorption and using a two-state all-or-nothing unfolding process might seem a little simplistic. While, to be more realistic, our model could certainly benefit from some enhancement regarding this point, this simple transition may approximate some protein behaviors when studying the general effects of an unfolding event. Indeed, in several cases, mostly for high molecular weight proteins, the three-dimensional structure of adsorbed proteins may be described as two overall states, compact and extended. This is, for instance, the case for fibronectin [22,48–50]. Fibronectin is a high molecular weight protein of the extracellular matrix of connective tissues in which it is found under a fibrillar form. The underlying assembly mechanisms are still under investigation but it has been shown that fibronectin fibrillogenesis may be surface induced [48,51,52]. Figure 6 presents a staining of human fibronectin adsorbed onto a bone substitute material,

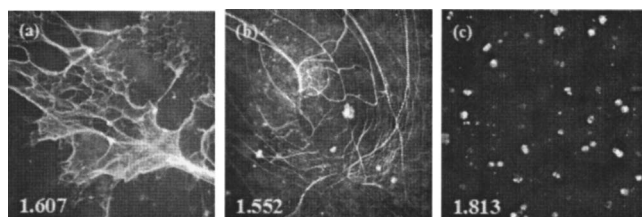


FIG. 6. Immunofluorescent staining of a fibronectin layer spontaneously formed upon adsorption onto (a), (b) hydroxyapatite or (c) cell culture glass. The cluster fractal dimension, estimated from a box counting method, is indicated at the bottom left of each picture. Each image is  $300 \times 300 \mu\text{m}$ .

hydroxyapatite (HA). Adsorption onto HA spontaneously induces fibronectin fibrillogenesis and produces large connected fibrillar structures the fractal dimension of which ranges over 1.5–1.6 [Figs. 6(a) and 6(b)]. Moreover, unlike classical DLA clusters, fibronectin clusters do not present an open ramified treelike structure but rather contain closed-loop structures inside the aggregates. All these features are captured by our model, in the DL regime for low unfolding probability [Figs. 3(a) and 3(b),  $P=10^{-6}$ ] or in the RL regime at higher unfolding probability [Fig. 4(a),  $P>10^{-5}$ ; Fig. 4(b),  $P=10^{-5}$ ], both when clustered unfolding is allowed.

The conformation change of a protein strongly depends on the surface it is adsorbed on [22,53–55] and our model allows the investigation of several protein-substrate couples. For instance, fibronectin adsorption onto glass leads to the formation of small compact aggregates [Fig. 6(c)], rather than to the fibrillar clusters observed on hydroxyapatite. These structures are similar to RLA aggregates and our model indicates that the difference with the adsorption structures observed on HA might reflect a difference in the protein unfolding on the two surfaces.

In addition to the surface-protein interaction, it is inferred from many experiments that protein interactions themselves play a major role in the conformational change, by either favoring or preventing it. The latter may be intuitively understood in terms of surface crowding [56–58]. This crowding may, however, have the opposite effect as exemplified by a number of data sets in the literature. For instance, adsorption-induced denaturation of lysozyme increases with increasing surface coverage, whatever the kind of surface [59]. Moreover, in the assembly of some specific protein structures, such as amyloid fibrils, conformational changes

occur concomitantly with aggregation [60,61]. The ability of a native protein to form such structures when seeded by preformed fibrils [62,63] suggests again that unfolded conformations may be stabilized by interactions with their neighbors. These aggregation mechanisms could actually be appropriate to many other proteins, since the hypothesis that most proteins would have an amyloidogenic potential has emerged [64,65]. The neighbor-required unfolding might ultimately be relevant to oligomerization mechanism such as domain swapping [66,67]. Taken together these results strongly suggest that neighbor-required unfolding might govern several protein aggregation processes.

Unfolding has significant impact on diffusive aggregation cluster morphology. Contrary to general diffusive aggregation models, rather leading to open branched structures, it allows the formation of looped structures, a feature shared by some protein fibrillar assemblies [19,51,52]. Despite and because of its simplicity, our model is relevant to general protein adsorption features as well as specific protein-protein interactions that may be inferred from experimental observations. We aim at improving the algorithm which is currently quite CPU time consuming to investigate some singular protein aggregative behavior. We study here the case where aggregation induces unfolding; the events might occur the other way round and conformational changes may surely alter the sticking and unfolding-inductive properties of a protein. Further investigation of the model will include different sticking properties depending on homotypic or heterotypic contacts between folded and unfolded monomers. We believe this might describe some experimental features such as the simultaneous growth of amorphous aggregates and fibrillar structures that is observed for some proteins at interfaces.

- 
- [1] V. Ball and J.-C. Voegel, *l'actualité chimique* **10**, 11 (2003).  
 [2] C. Combes and C. Rey, *Biomaterials* **23**, 2817 (2003).  
 [3] F. Cuisinier, *Curr. Opin. Solid State Mater. Sci.* **1**, 436 (1996).  
 [4] G. K. Hunter, *Curr. Opin. Solid State Mater. Sci.* **1**, 430 (1996).  
 [5] J. Kirkham *et al.*, *Curr. Opin. Colloid Interface Sci.* **7**, 124 (2002).  
 [6] N. L. Harris *et al.*, *Bone (N.Y.)* **27**, 795 (2000).  
 [7] D. Couchourel *et al.*, *J. Inorg. Biochem.* **73**, 129 (1999).  
 [8] G. Daculsi, P. Pilet, M. Cottrel, and G. Guicheux, *J. Biomed. Mater. Res.* **47**, 228 (1999).  
 [9] T. Saito *et al.*, *Bone (N.Y.)* **21**, 305 (1997).  
 [10] R. Fujisawa, Y. Wada, Y. Nodasaka, and Y. Kuboki, *Biochim. Biophys. Acta* **1292**, 53 (1996).  
 [11] G. K. Hunter *et al.*, *Biochem. J.* **317**, 59 (1996).  
 [12] J. J. Gray, *Curr. Opin. Struct. Biol.* **14**, 110 (2004).  
 [13] A. Rosengren *et al.*, *Biomaterials* **24**, 147 (2003).  
 [14] A. Gessner, A. Lieske, B. R. Paulke, and R. H. Muller, *Eur. J. Pharm. Biopharm.* **54**, 165 (2002).  
 [15] A. Rosengren *et al.*, *Biomaterials* **23**, 1237 (2002).  
 [16] A. Kotwal and C. E. Schmidt, *Biomaterials* **22**, 1055 (2001).  
 [17] D. E. Mc Donald, B. Markovic, A. L. Boskey, and P. Somasundaran, *Colloids Surf., B* **11**, 131 (1998).  
 [18] M. F. M. Engel, C. P. M. Van Mierlo, and A. J. G. W. Wissers, *J. Biol. Chem.* **277**, 10922 (2002).  
 [19] J. S. Sharp, J. A. Forrest, and R. A. L. Jones, *Biochemistry* **41**, 15810 (2002).  
 [20] S. S. Karajanagi, A. A. Vertegel, R. S. Kane, and J. S. Dordick, *Langmuir* **20**, 11594 (2004).  
 [21] W. Norde and T. Zoungrana, *Biotechnol. Appl. Biochem.* **28**, 133 (1998).  
 [22] L. Bough and V. Vogel, *J. Biomed. Mater. Res.* **69**, 525 (2004).  
 [23] D. J. Iuliano, S. S. Saavedra, and G. A. Truskey, *J. Biomed. Mater. Res.* **27**, 1103 (1993).  
 [24] L. Kam and S. G. Boxer, *J. Biomed. Mater. Res.* **55**, 487 (2001).  
 [25] M. Mrksich *et al.*, *Proc. Natl. Acad. Sci. U.S.A.* **93**, 10775 (1996).  
 [26] G. Maheshwari *et al.*, *J. Cell. Sci.* **113**, 1677 (2000).  
 [27] T. A. Witten and L. M. Sander, *Phys. Rev. Lett.* **47**, 1400 (1981).  
 [28] P. Jensen *et al.*, *Chaos, Solitons Fractals* **6**, 227 (1995).  
 [29] S. Ravichandran and J. Talbot, *Biophys. J.* **78**, 110 (2000).  
 [30] M. Zhu *et al.*, *J. Biol. Chem.* **277**, 50914 (2002).  
 [31] I. Pallarès, J. Vendrell, F. X. Avilès, and S. Ventura, *J. Mol. Biol.* **342**, 321 (2004).



- [32] V. N. Uversky and A. L. Fink, *Biochim. Biophys. Acta* **1698**, 131 (2004).
- [33] R. Khurana *et al.*, *Biochemistry* **40**, 3525 (2001).
- [34] J. W. Kelly, *Curr. Opin. Struct. Biol.* **6**, 11 (1996).
- [35] P. R. Van Tassel *et al.*, *J. Colloid Interface Sci.* **207**, 317 (1998).
- [36] Y. Tie, A. P. Ngankam, and P. R. Van Tassel, *Langmuir* **20**, 10599 (2004).
- [37] Y. Tie, C. Calonder, and P. R. Van Tassel, *J. Colloid Interface Sci.* **268**, 1 (2003).
- [38] G. J. Szöllösi, I. Derényi, and J. Vörös, *Physica A* **343**, 359 (2004).
- [39] C. F. Wertz and M. M. Santore, *Langmuir* **18**, 706 (2002).
- [40] J. G. Amar and F. Family, *Phys. Rev. B* **50**, 8781 (1994).
- [41] P. Jensen *et al.*, *Phys. Rev. B* **50**, 15316 (1994).
- [42] S. Buczowski, S. Kyriacos, F. Nekka, and L. Cartilier, *Pattern Recogn.* **31**, 411 (1998).
- [43] P. Meakin, *Phys. Rev. Lett.* **51**, 1119 (1983).
- [44] A. M. Puertas, A. Fernandez-Barbero, F. Javier de la Nieves, and L. F. Rull, *Langmuir* **20**, 9861 (2004).
- [45] J. Parkinson, K. E. Adler, and A. Brass, *J. Mol. Biol.* **247**, 823 (1995).
- [46] J. Parkinson, K. E. Adler, and A. Brass, *Phys. Rev. E* **50**, 2963 (1994).
- [47] A. Mohraz, D. B. Moler, R. M. Ziff, and M. J. Solomon, *Phys. Rev. Lett.* **92**, 155503 (2004).
- [48] M. Bergkvist, J. Carlsson, and S. Oskarsson, *J. Biomed. Mater. Res.* **64**, 349 (2003).
- [49] M. Raghavachari, H-M Tsai, K. Kottke-Marchant, and R. E. Marchant, *Chin. Sci. Bull.* **19**, 315 (2000).
- [50] N. M. Tooney *et al.*, *J. Cell Biol.* **97**, 1686 (1983).
- [51] N. Pernodet *et al.*, *J. Biomed. Mater. Res.* **64**, 684 (2003).
- [52] D. Pellenc *et al.* (unpublished).
- [53] A. Agnihotri and C. A. Siedlecki, *Langmuir* **20**, 8846 (2004).
- [54] W. Hoyer, D. Cherny, V. Subramaniam, and T. M. Jovin, *J. Mol. Biol.* **340**, 127 (2004).
- [55] M. Tanaka *et al.*, *Colloids Surf., A* **203**, 195 (2002).
- [56] P. Y. Meadows, J. E. Bemis, and G. C. Walker, *Langmuir* **19**, 9566 (2003).
- [57] A. Kondo and H. Fukuda, *J. Colloid Interface Sci.* **198**, 34 (1998).
- [58] A. Kondo and J. Mihara, *J. Colloid Interface Sci.* **117**, 214 (1996).
- [59] A. Sethuraman *et al.*, *Proteins* **56**, 669 (2004).
- [60] A. J. Modler, K. Gast, G. Lutsch, and G. Damaschun, *J. Mol. Biol.* **325**, 135 (2003).
- [61] T. Scheibel, J. Bloom, and S. L. Lindquist, *Proc. Natl. Acad. Sci. U.S.A.* **101**, 2287 (2003).
- [62] Y. Xing *et al.*, *J. Biol. Chem.* **277**, 33164 (2002).
- [63] M. R. H. Krebs *et al.*, *J. Mol. Biol.* **300**, 541 (2000).
- [64] X. Fu *et al.*, *FEBS Lett.* **563**, 179 (2004).
- [65] C. M. Dobson, *Trends Biochem. Sci.* **24**, 329 (1999).
- [66] F. Rousseau, J. W. H. Schymkowitz, and L. S. Itzhaki, *Structure (London)* **11**, 243 (2003).
- [67] M. E. Newcomer, *Curr. Opin. Struct. Biol.* **12**, 48 (2002).